Supporting Information

A Holey 2D MoS_2-based Membrane with Mo-rich Edges for Water Desalination

Biswajit Mondal[1], Sudhin Rathnakumaran[2], Amrita Chakraborty[1,4], Pragin Chettiyankandy[2], Pillalamarri Srikrishnarka[1], Md Rabiul Islam[1], Jenifer Shantha Kumar[1], Ramesh Kumar[1], Sandeep Bose[1], Sooraj Kunnikuruvan[2,3] and Thalappil Pradeep[1]**

[1]DST Unit of Nanoscience (DST UNS) and Thematic Unit of Excellence (TUE), Department of Chemistry, Indian Institute of Technology Madras, Chennai – 600036, India.

[2]Department of Chemistry, Indian Institute of Technology Madras, Chennai – 600036, India

[3]Centre for Atomistic Modelling and Materials Design & Centre for Molecular Materials and Functions, Indian Institute of Technology Madras, Chennai – 600036, India

[4]Department of Chemistry, BITS Pilani Hyderabad Campus, Telangana 500078, India

*E-mail: pradeep@iitm.ac.in

soorajk@iitm.ac.in

Table of contents

EXPERIMENTAL SECTION

Chemicals: All the commercially available chemicals were used without further purification. Silver acetate (AgOAc), molybdenum disulfide (MoS_2), 1.6 M n-butyllithium in hexane, camphorsulfonic acid, sodium lauryl sulfate (SLS), and 1,3,5-Benzenetricarbonyl trichloride (TMC) were purchased from Sigma Aldrich, India. All the solvents hexane and N-Methyl-2-pyrrolidone were used without further purification.

Synthesis of MoS_2 NS: MoS_2 NSs were synthesized using the chemical exfoliation method from bulk MoS_2 powder. In the typical synthesis, 300 mg of MoS_2 powder was taken in a round bottom flask, under argon atmosphere, and 3 mL of 1.6 M n-butyllithium was added. The resulting solution was stirred for 2 days under the same inert conditions. Then the resulting

lithium-intercalated product was washed repeatedly with hexane, to remove excess n-butyllithium. Then, it was centrifuged to collect cleaned lithium-intercalated product and 100 mL of distilled water was added to it. The product was sonicated in a bath sonicator for 1 h to get exfoliated MoS_2 NS. This aqueous dispersion of MoS_2 NSs was centrifuged at a speed of 18000 rpm to remove un-exfoliated MoS_2. The quality of the synthesized MoS_2 NSs was checked using electron microscopy, UV-Vis, and Raman spectroscopy.

Preparation of Mo-rich holey MoS_2 NS: For electrospray deposition of Ag^+ ions, a home-built nanoelectrospray ionization (nESI) source was used. The nESI source was made by pulling a borosilicate glass capillary (0.86 mm ID and 1.5 mm OD) into two, using a micropipette puller (Sutter Instruments, U.S.A.). Each tip, after pulling, was checked using an optical microscope to ensure the size and quality of the cut. Tips with an opening of 10-15 µm were used for the electrospray deposition of Ag^+ ions. 10 mM aqueous solution of AgOAc was filled in the nESI tips using a microinjector pipette tip and Pt wire was inserted into the solution, making an electrode for high voltage connection. For electrospray deposition on MoS_2 NSs, an aqueous suspension of MoS_2 NS was taken in an Eppendorf vial and the Ag^+ ions were guided towards it. The aqueous MoS_2 suspension was grounded through a picoammeter using a copper strip. The pore size is primarily governed by the deposition time. We attempted to control the pore size by varying the deposition duration; however, for a fixed deposition time, no significant variation in pore size was observed. The sizes of the nanopores were further checked using transmission electron microscope.

Fabrication of membranes: Membranes were fabricated using an easy and cost-effective co-polymerization method. In the first step, a solution of polysulfone (psf) in NMP was coated on a polyester non-woven fabric and immediately, it was dipped into water. Then, a mixture of solutions of holey MoS_2 NS, MPD, SLS, and camphorsulfonic acid was added to psf-coated polyester non-woven fabric. Then the solution was carefully drained off after a certain time. A solution of TMC in hexane was added and kept in contact for a certain time. The solution was

drained off and then the membrane was dried inside an oven at 60 ^{o}C. The concentration of all the reagents and the contact time of both solutions were optimized.

Test of performance of the membranes: The performance of the membranes was tested using RO membrane test skid. All the experiments were done at a pressure of 20 bar (except "pressure dependent flux" experiment) and the TDS of feed water was 2000 ppm. The pressure-dependent experiments were done in the pressure range of 5 bar to 40 bar. Photograph of test skid is shown in Figure S3.

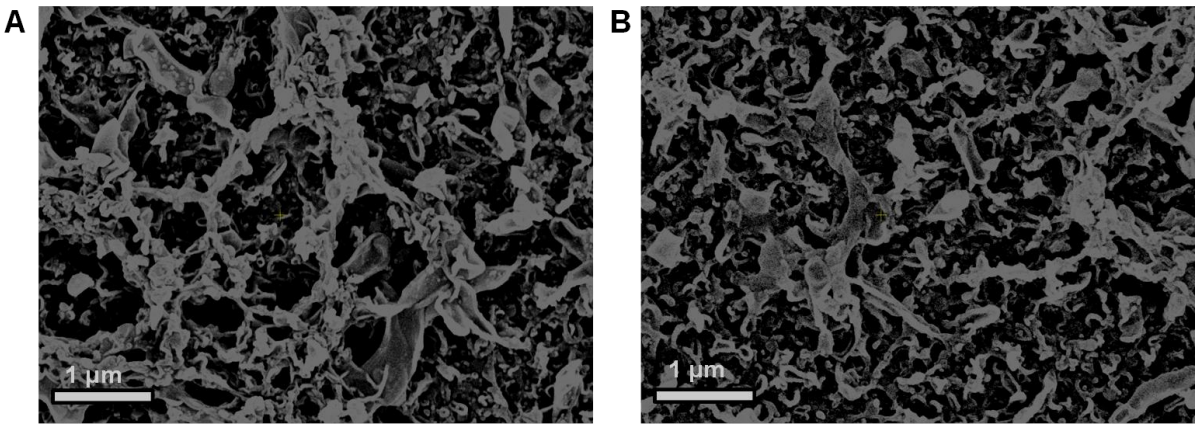

Figure S1. FESEM images of hMoS_2M (A) and MoS_2M (B).

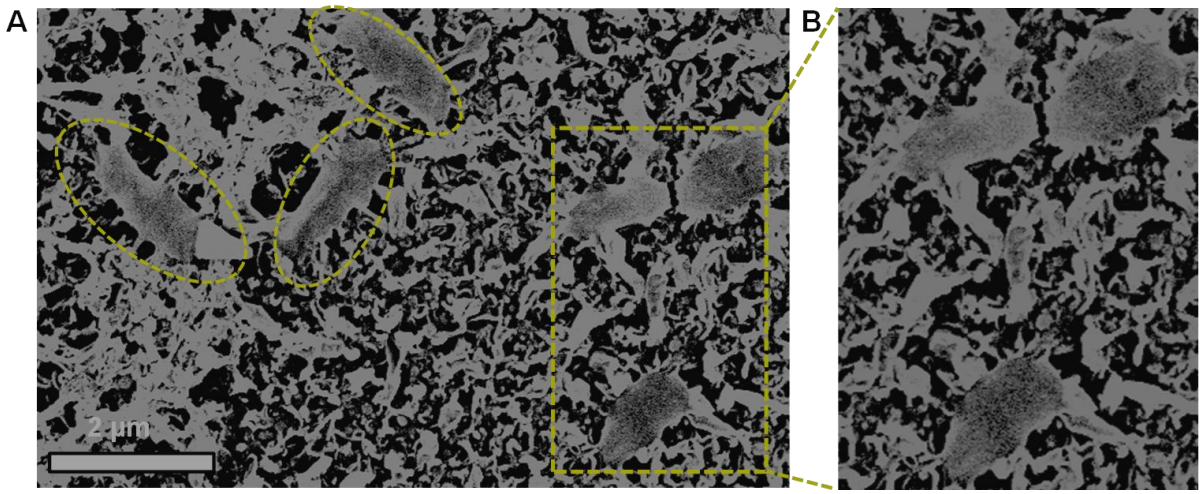

Figure S2. FESEM images of 0.015 wt% hMoS_2M showing agglomeration of MoS_2 NSs.

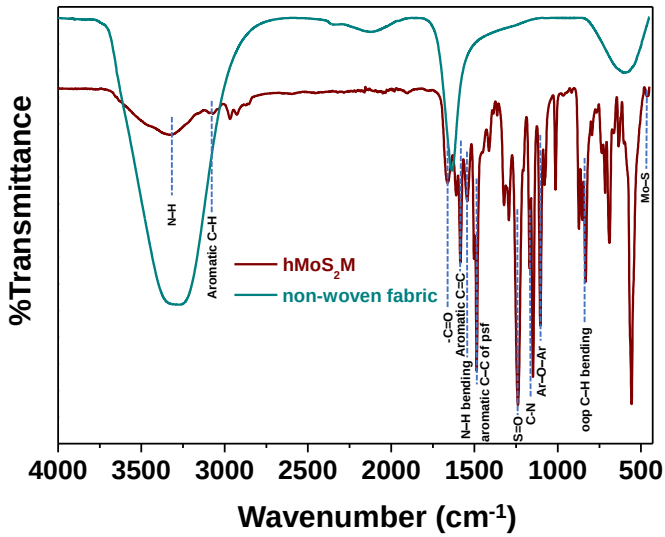

Figure S3. The FT-IR spectrum of hMoS$_2$M confirms the presence of all characteristic peaks associated with PA and MoS$_2$.

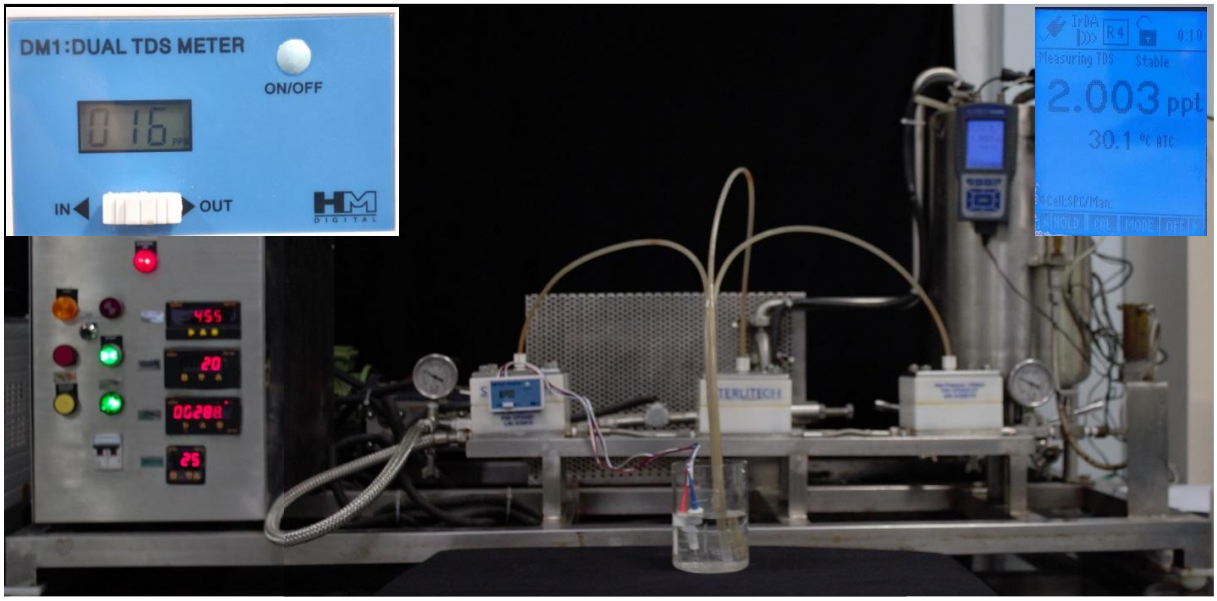

Figure S4. Photograph of the set-up used to test the performance of the membranes.

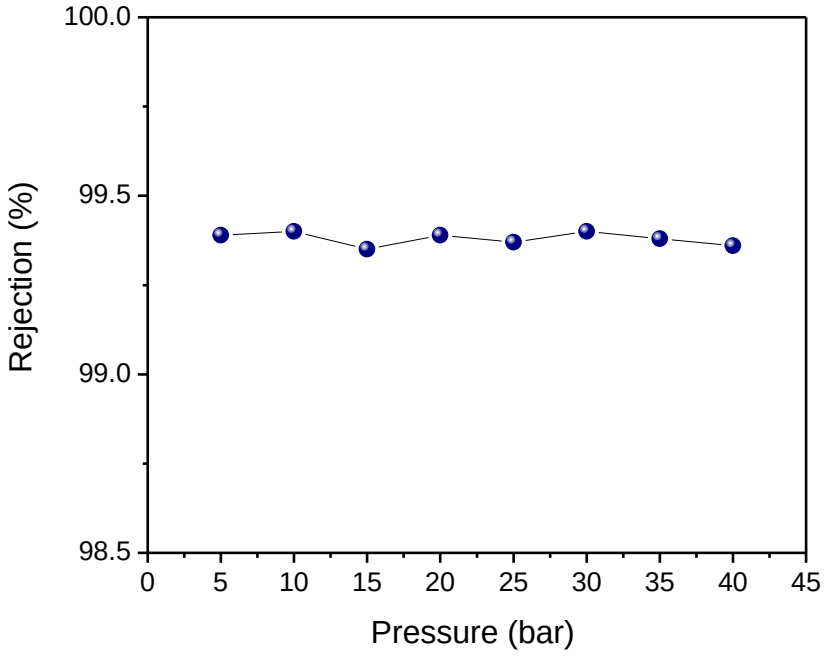

Figure S5. Pressure-dependent ion rejection performance of holey MoS_2-based membrane.

Computational details:

The MoS_2 NSs were constructed using the CHARMM-GUI Nanomaterial Modeler.[1] The PA oligomer structure (Figure S5) was prepared based on a previous study,[2] which reports a degree of crosslinking (DC) of about 71%. The cross-linked PA oligomer was formed via condensation between 11 MPD and 10 TMC monomers. To build the membrane models for MD simulations, five such PA oligomers were placed on either side of the hMoS_2NSs in a sandwiched configuration. This initial molecular arrangement was generated using PACKMOL.[3] At both ends of the system, graphene pistons were placed. Periodic boundary conditions (PBC) were applied, and a vacuum layer of 10 nm was added in the Z-direction to avoid interactions between the periodic images.

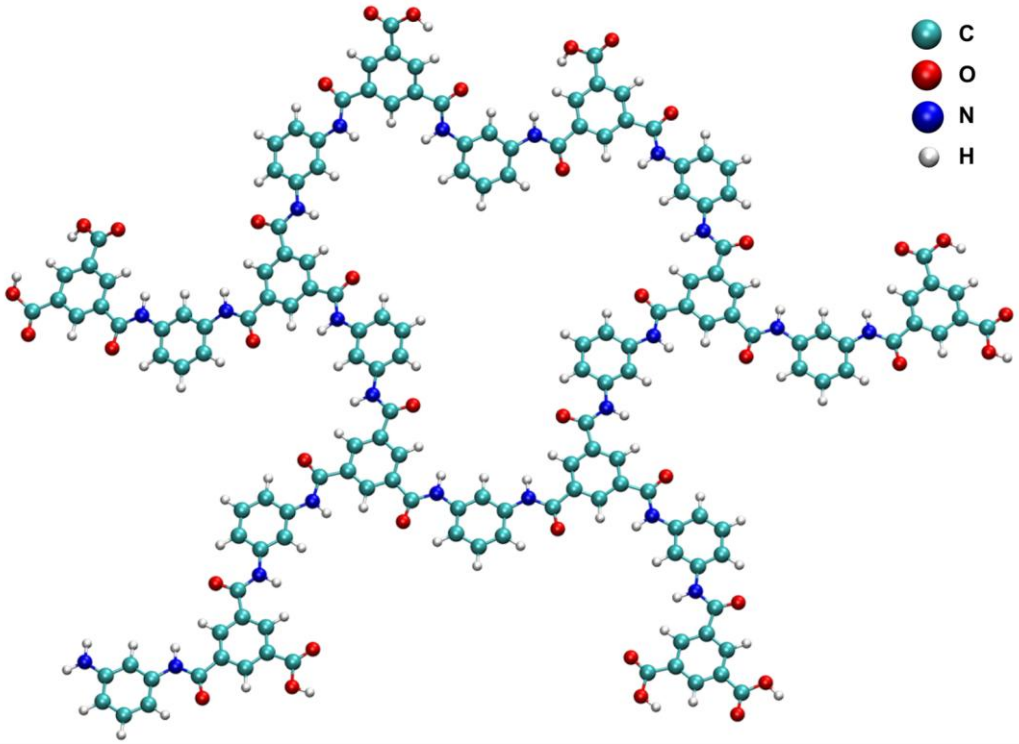

Figure S6: Optimized structure of the PA oligomer used in the MD simulations.

The TIP3P water model was used here,[4] and the SHAKE algorithm with a tolerance of 0.0001 was employed to constrain bond lengths and angles of water molecules.[5] The Lennard-Jones (LJ) parameters for Mo, S, Na, and Cl were adopted from a previous study.[6] The Mo and S atoms were assigned atomic charges of +0.5 and -0.25, respectively.[7] The PA oligomers were described using the DREIDING force field,[8] with atomic charges derived from electrostatic potential (ESP) charges calculated on the monomer unit (Figure S6 and Table S1) using the Gaussian 16 suite of programs at the B3LYP/6-311++G(d,p) level of theory.[9] All the other LJ parameters for the pairwise interactions were computed using the Lorentz-Berthelot mixing rules. A cutoff distance of 12 Å was used for both LJ and Coulombic interactions. Long-range Coulombic interactions were treated using the particle-particle particle-mesh (PPPM) method implemented in LAMMPS, with a relative root-mean-square (RMS) error of 0.0001 in the forces.

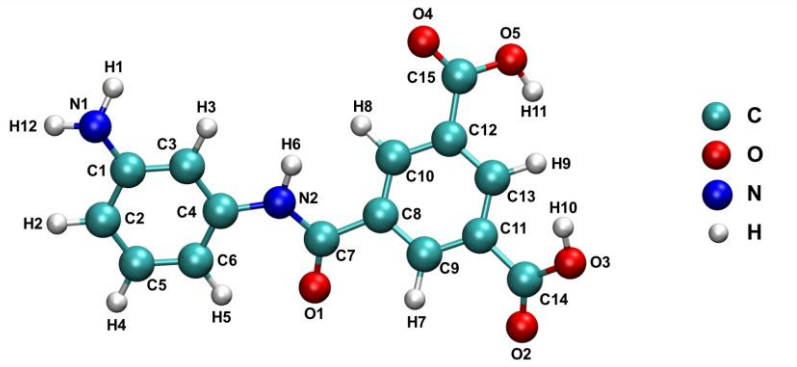

Figure S7: Optimized structure of the PA monomer used for the ESP charge calculations.

Table S1: Calculated ESP charges for atoms of the PA monomer. Atom labels are consistent with Figure S7.

Atom	ESP charge (*e*)
C1	0.4
C2	-0.33
C3	-0.53
C4	-0.1
C5	0.59
C6	-0.36
C7	0.7
C8	-0.07
C9	-0.03
C10	-0.03
C11	-0.19
C12	-0.19
C13	-0.08
C14	0.74

C15	0.74
H1	0.33
H2	0.18
H3	0.23
H4	0.15
H5	0.2
H6	0.3
H7	0.12
H8	0.12
H9	0.11
H10	0.4
H11	0.4
H12	0.33
N1	-0.75
N2	-0.73
O1	-0.51
O2	-0.48
O3	-0.58
O4	-0.48
O5	-0.58

Initially, energy minimization was performed on the RO setup, setting the relative energy tolerance to 10^{-8} and force tolerance to 10^{-10} kcal mol^{-1} $Å^{-1}$. The graphene pistons were constrained in the XY-plane, while the hMoS_2NSs were fixed in all three spatial dimensions. Following minimization, NPT and NVT equilibrations were performed at a temperature of 300

K and a pressure of 1 atm for 1 ns. RO simulations were then carried out on the equilibrated setup under the NVT ensemble at 300 K for 10 ns at each applied pressure. During the NVT equilibration and RO simulations, the pistons were subjected to the required amount of pressure (p) using forces applied in the Z-direction, calculated as:

$$F = \frac{pA}{N}$$

where F is the force per atom, A is the surface area of the piston, and N is the number of C atoms in the piston. For the NVT equilibration runs, the pistons were maintained at a pressure of p = 1 atm. During the RO simulations, pressures of p = 50 to 300 MPa with an interval of 50 MPa were applied to the piston on the feed side, while the piston on the permeate side was kept at p = 1 atm. A time step of 1 fs was used in all these simulations. The equilibrated RO setups within the periodic simulation boxes are shown in Figure S7.

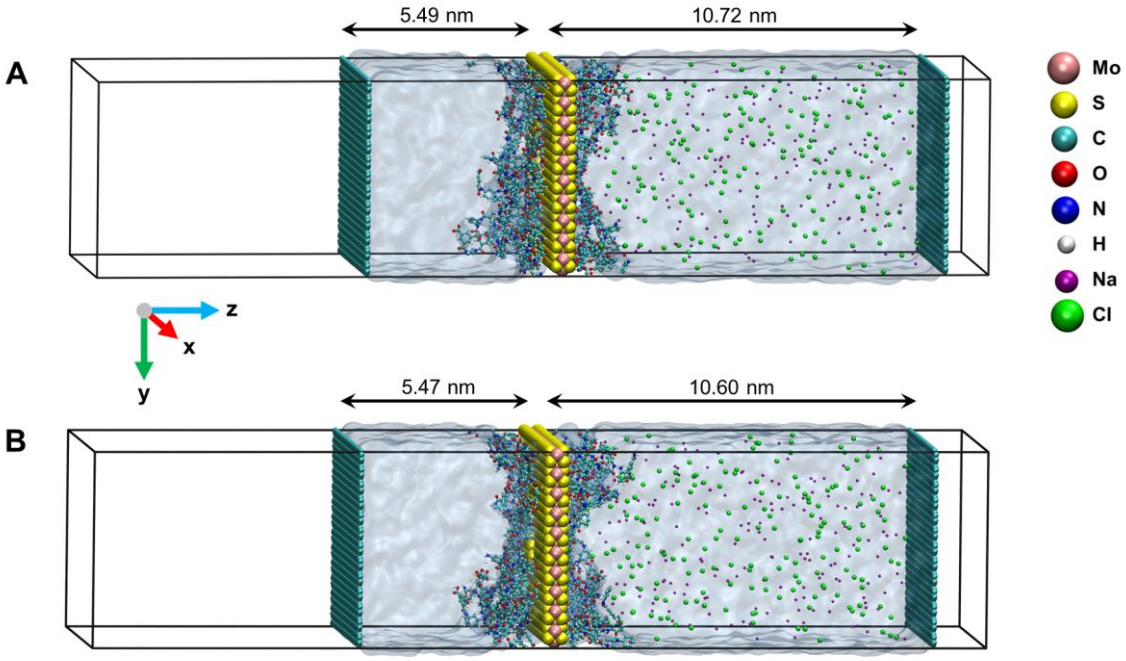

Figure S8. Periodic simulation boxes used in the RO simulations showing the feed and permeate layer sizes for the (A) Mo-rich and (B) S-rich hMoS_2Ms.

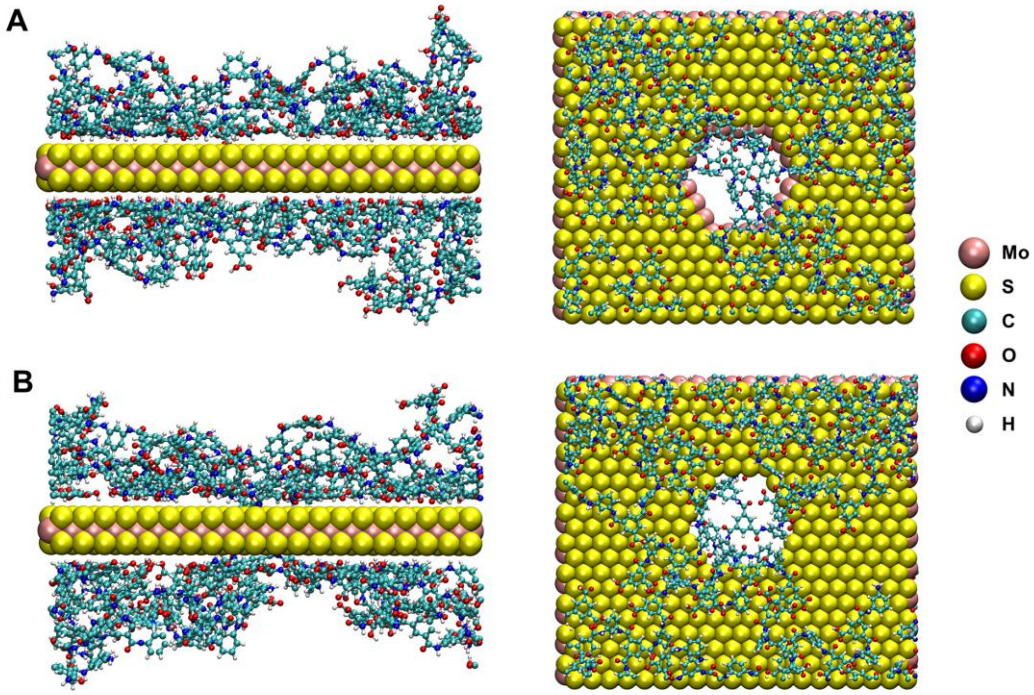

Figure S9. Equilibrated membrane structures (side and top views) of (A) Mo-rich and (B) S-rich $hMoS_2Ms$.

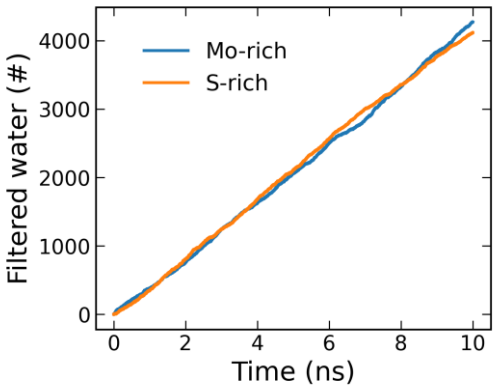

Figure S10: Number of filtered water molecules as a function of simulation time for the Mo-rich and S-rich $hMoS_2Ms$ at an applied pressure of 200 MPa.

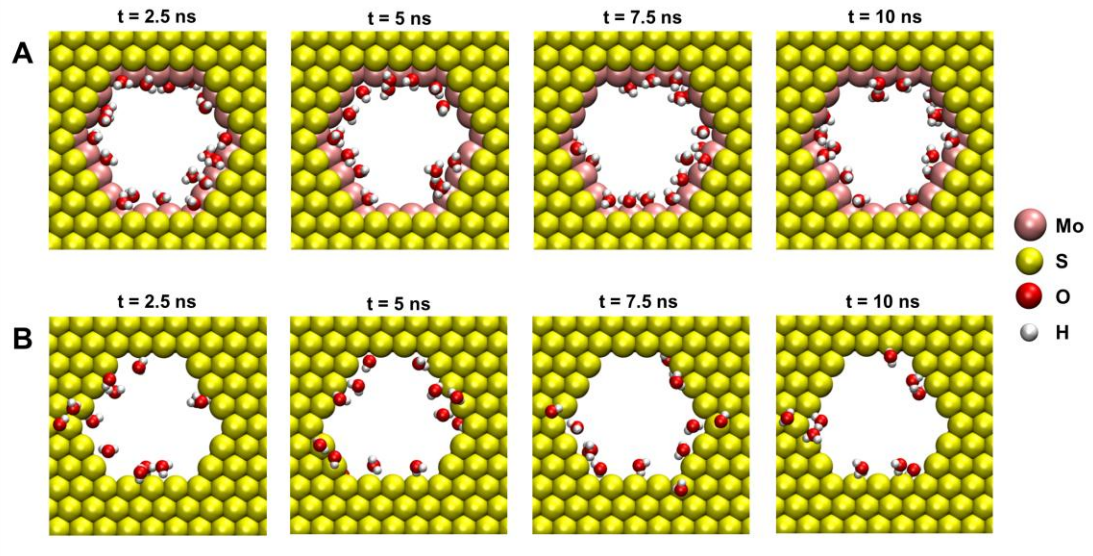

Figure S11. Snapshots showing the pore region and water molecules within 3.3 Å of the pore atoms for (A) Mo-rich $hMoS_2M$ and (B) S-rich $hMoS_2M$ from RO simulations performed at 200 MPa.

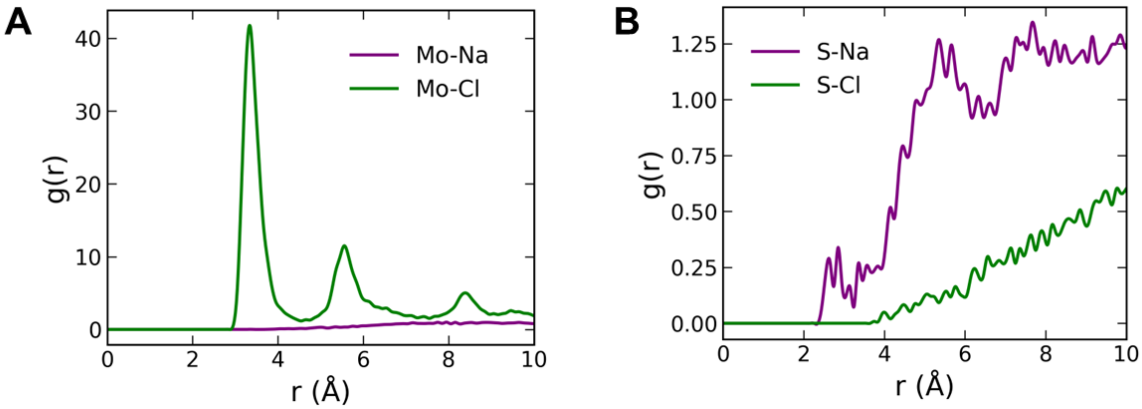

Figure S12. RDF plots between (A) salt ions and Mo atoms, and (B) salt ions and S atoms for the Mo-rich and S-rich $hMoS_2Ms$, computed from RO simulations at 200 MPa.

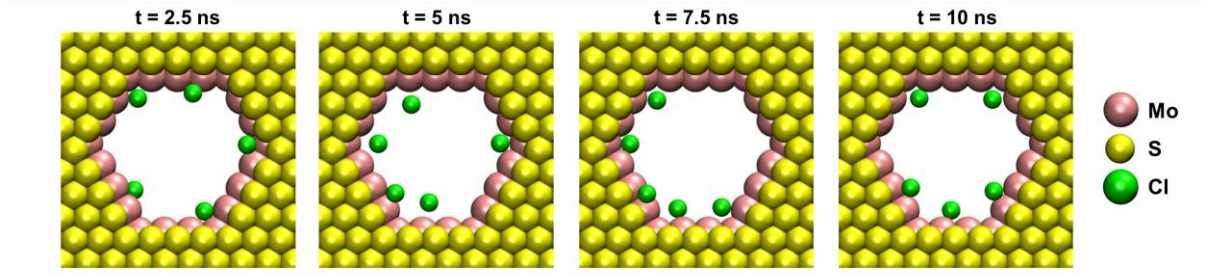

Figure S13. Snapshots showing the pore region and Cl^- ions within 4 Å of the pore Mo atoms for Mo-rich $hMoS_2M$ from RO simulation performed at 200 MPa.

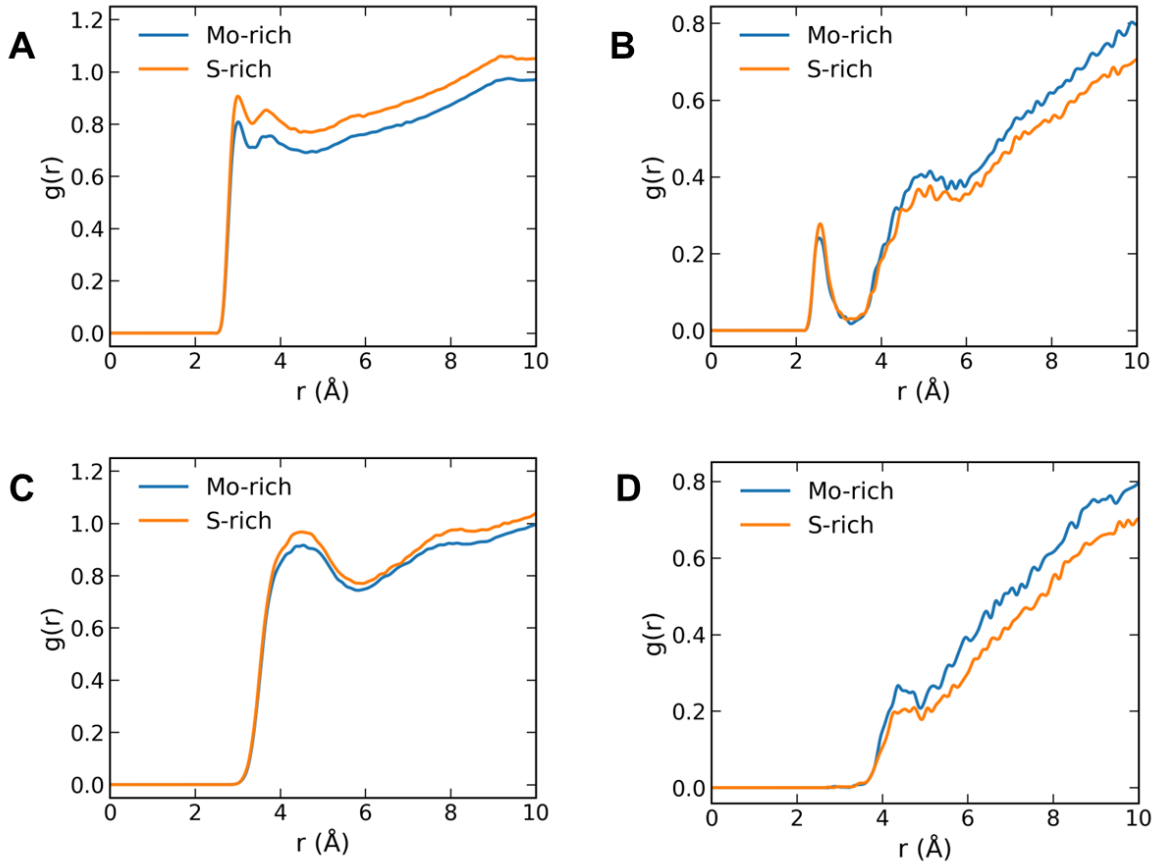

Figure S14. RDF plots between (A) O of PA and O of water, (B) N of PA and O of water, (C) O of PA and salt ions, and (D) N of PA and salt ions, for the Mo-rich and S-rich $hMoS_2Ms$, computed from RO simulations at 200 MPa.

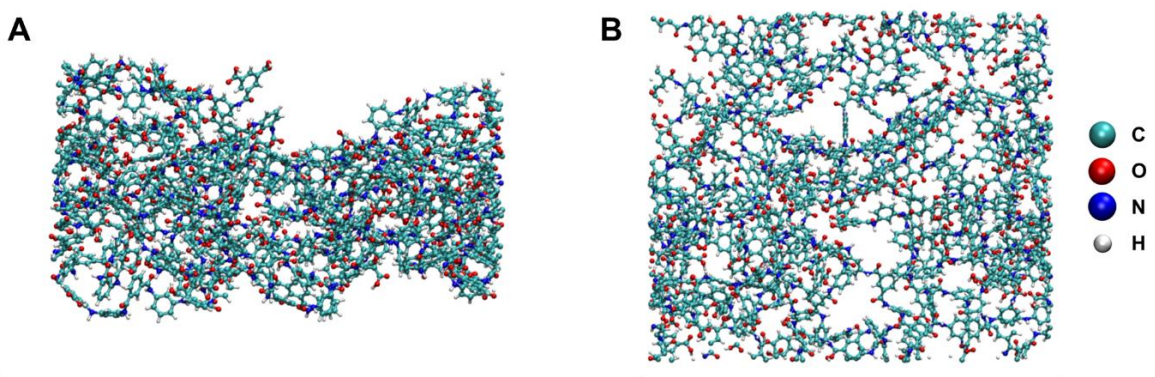

Figure S15. (A) Side and (B) top views of the equilibrated bM structure composed solely of PA oligomers.

Computational data and code availability:

The LAMMPS input and data files used for the MD simulations in this work are available at:

https://drive.google.com/drive/folders/1DZeFyLgIpvCdsc9hmNEi0Ab6TFPKMO1Y

References

(1) Choi, Y. K.; Kern, N. R.; Kim, S.; Kanhaiya, K.; Afshar, Y.; Jeon, S. H.; Jo, S.; Brooks, B. R.; Lee, J.; Tadmor, E. B.; Heinz, H.; Im, W. CHARMM-GUI Nanomaterial Modeler for Modeling and Simulation of Nanomaterial Systems. *J Chem Theory Comput* **2022**, *18* (1), 479–493. https://doi.org/10.1021/acs.jctc.1c00996.

(2) Yoshioka, T.; Kotaka, K.; Nakagawa, K.; Shintani, T.; Wu, H.-C.; Matsuyama, H.; Fujimura, Y.; Kawakatsu, T. Molecular Dynamics Simulation Study of Polyamide Membrane Structures and RO/FO Water Permeation Properties. *Membranes (Basel)* **2018**, *8* (4), 127. https://doi.org/10.3390/membranes8040127.

(3) Martínez, L.; Andrade, R.; Birgin, E. G.; Martínez, J. M. PACKMOL: A Package for Building Initial Configurations for Molecular Dynamics Simulations. *J Comput Chem* **2009**, *30* (13), 2157–2164. https://doi.org/10.1002/jcc.21224.

4) Price, D. J.; Brooks, C. L. A Modified TIP3P Water Potential for Simulation with Ewald Summation. *J Chem Phys* **2004**, *121* (20), 10096–10103. https://doi.org/10.1063/1.1808117.

(5) Andersen, H. C. Rattle: A "Velocity" Version of the Shake Algorithm for Molecular Dynamics Calculations. *J Comput Phys* **1983**, *52* (1), 24–34. https://doi.org/10.1016/0021-9991(83)90014-1.

(6) Wu, B.; Song, Z.; Xiang, Y.; Sun, H.; Yao, H.; Chen, J. Desalination Performance of MoS_2 Membranes with Different Single-Pore Sizes: A Molecular Dynamics Simulation Study. *ACS Omega* **2024**, *9* (21), 22851–22857. https://doi.org/10.1021/acsomega.4c01208.

(7) Sresht, V.; Govind Rajan, A.; Bordes, E.; Strano, M. S.; Pádua, A. A. H.; Blankschtein, D. Quantitative Modeling of MoS_2 –Solvent Interfaces: Predicting Contact Angles and Exfoliation Performance Using Molecular Dynamics. *The Journal of Physical Chemistry C* **2017**, *121* (16), 9022–9031. https://doi.org/10.1021/acs.jpcc.7b00484.

(8) Mayo, S. L.; Olafson, B. D.; Goddard, W. A. DREIDING: A Generic Force Field for Molecular Simulations. *J Phys Chem* **1990**, *94* (26), 8897–8909. https://doi.org/10.1021/j100389a010.

(9) Frisch, M. J.; Trucks, G. W.; Schlegel, H. B.; Scuseria, G. E.; Robb, M. A.; Cheeseman, J. R.; Scalmani, G.; Barone, V.; Petersson, G. A.; Nakatsuji, H.; Li, X.; Caricato, M.; Marenich, A. V; Bloino, J.; Janesko, B. G.; Gomperts, R.; Mennucci, B.; Hratchian, H. P.; Ortiz, J. V; Izmaylov, A. F.; Sonnenberg, J. L.; Williams-Young, D.; Ding, F.; Lipparini, F.; Egidi, F.; Goings, J.; Peng, B.; Petrone, A.; Henderson, T.; Ranasinghe, D.; Zakrzewski, V. G.; Gao, J.; Rega, N.; Zheng, G.; Liang, W.; Hada, M.; Ehara, M.; Toyota, K.; Fukuda, R.; Hasegawa, J.; Ishida, M.; Nakajima, T.; Honda, Y.; Kitao, O.; Nakai, H.; Vreven, T.; Throssell, K.; Montgomery Jr., J. A.; Peralta, J. E.; Ogliaro, F.; Bearpark, M. J.; Heyd, J. J.; Brothers, E. N.; Kudin, K. N.; Staroverov, V. N.; Keith, T. A.; Kobayashi, R.; Normand, J.; Raghavachari, K.; Rendell, A. P.; Burant, J. C.; Iyengar, S. S.; Tomasi, J.; Cossi, M.; Millam, J. M.; Klene, M.; Adamo, C.; Cammi, R.; Ochterski, J. W.; Martin, R. L.; Morokuma, K.; Farkas, O.; Foresman, J. B.; Fox, D. J. Gaussian 16, Revision C.01. 2016.